

Nanostructure Polyaniline (PANI) Decorated TiO₂ Nanocomposite as Efficient Heterogeneous Catalyst

Kalpna N. Handore^{1,*}, Sumit Sharma², Smita Jagtap³, Vasant V. Chabukswar³, M.J. Sable⁴, R.A. Gujar⁵ and S.H. Gawande^{6,*}

¹Department of Chemistry, Marathwada Mitramandal's College of Engineering, Karvenagar Pune, India

²Department of Chemistry, Modern Education Society's Wadia College of Engineering, S. P. Pune University, Pune, India

³Department of Chemistry, Nowrosjee Wadia College, S. P. Pune University, Pune, Maharashtra, India

⁴Department of Mechanical Engineering, COEP Technological University, Wellesley Rd, Shivajinagar, Pune, India

⁵Department of Mechanical Engineering, Pimpri Chinchwad College of Engineering, S. P. Pune University, Pune, India

⁶Industrial Tribology Laboratory, Department of Mechanical Engineering, Modern Education Society's Wadia College of Engineering, S. P. Pune University, Pune, India

Abstract: The paper describes the synthesis of conducting polyaniline-TiO₂ (PANI-TiO₂) nanocomposite by chemical oxidative polymerization method using aniline as a monomer. TiO₂ nanoparticles were synthesized by sol gel method using TiCl₄ and ethanol. Ultrasound synthesized TiO₂ nanoparticles and nanocomposite were characterized by various spectroscopic techniques UV, FT-IR, XRD, SEM and TGA. The XRD pattern confirms the appearance of sharp diffraction patterns indicating the small sized, high purity TiO₂ nano particles are highly agglomerated with spherical morphology. The PANI-TiO₂ nanocomposite was employed as a promising heterocyclic, reusable catalyst for most of the organic synthesis. The advantages of this methodology are mild reaction conditions with short reaction time, excellent yields, low loading and reusability of catalyst.

Keywords: PANI-TiO₂, Solgel method, Nanocomposite, Biologically active, Ultrasound, DHPM.

1. INTRODUCTION

Organic synthesis focusses on the development of multiple bonds forming transformation allowing the creation of several covalent bonds in a single operation. Hence, the number of steps required for obtaining the target molecules is reduced which addresses the economy and efficiency criteria of green route chemistry. The Biginelli reaction is a well-known multi-component reaction involving one pot cyclo-condensation of aldehydes, β -keto ester and urea under strong acidic conditions [1,2]. A major drawback of Biginelli's reaction is low yields in the case of substituted aromatic and aliphatic aldehydes. Dihydropyrimidinones (DHPM's) and its derivatives, which are well known for their wide range of pharmacological profiles [3,4] like antiviral, alpha antagonists, neuropeptide (NPY) antagonists, antihypertensive, anti-inflammatory, antibacterial,

calcium channel blocker [5,6] etc. and having various other applications in the field of drug research have stimulated the invention of a wide range of developed synthetic routes. Several alkaloids containing a dihydropyrimidinone and thiones core have been isolated from marine sources, which show strong biological activity. Solvent-free organic reactions have been applied as a useful protocol in organic synthesis. Solvent-free conditions often lead to shorter reaction times, increased yields, easier workup that matches with green chemistry protocols and may enhance the regio-and stereo selectivity of reactions [7,8].

Among the conducting polymers, polyaniline and polyindole are often used as an organic part to prepare nanocomposites because of their low cost, ease in preparation, controllable unique properties by oxidation and protonation state, excellent environmental stability and potential applications in electronic devices. A number of different metal oxide particles have so far been encapsulated into the shell of polyaniline giving rise to a host of nanocomposites. Various reusable conducting polymeric material are used as a catalyst such as polyaniline [9] and polyaniline nanocomposite for electrochemical water splitting and dyes

*Address corresponding to these authors at the Department of Chemistry, Marathwada Mitramandal's College of Engineering, Karvenagar Pune, India; E-mail: kalpanahandore@mmcoe.edu.in

Industrial Tribology Laboratory, Department of Mechanical Engineering, Modern Education Society's Wadia College of Engineering, S. P. Pune University, Pune, India; E-mail: shgawande@gmail.com

degradation [10]. Polyindole and nanocomposite shows best catalytic, antibacterial activity [11-17] and anticorrosive properties [18-19]. Polymer nanocomposites can also be used in textiles [20].

Titanium dioxide (TiO₂) is attractive owing to its superior properties such as high photocatalytic activity, excellent stability, super-hydrophilicity, non-toxicity, biological and chemical inertness, semiconductor and optoelectronic properties [21-22]. Electrical and optical properties of titania (TiO₂) have been extensively employed in many fields such as solar cells, sensors [24], photo-catalysis [25] photovoltaic cells and photo-electrolysis as well as antibacterial [26], photo-chemical water purification [27], and self-cleaning applications.

Consequently, there is a scope for modification of reaction conditions and improving yields. From the literature survey, it is evident that there is a need to carry out this reaction with higher yield, low chemical loading and shorter reaction times under milder reaction conditions. The replacement of environmental hazardous solvents by solvent free conditions and catalysts (by the use of solid catalysts) are the innovative trends. In a continuation of our previous work on heterogeneous catalysts, we report a cheap, recoverable and efficient catalytic system for the synthesis of dihydropyrimidinones and thiones from aldehyde in the presence of PANI – TiO₂ nano catalyst.

The present study reports an efficient method for the synthesis of 3,4-dihydropyrimidin-2-(1H)-ones prepared via the condensation of aromatic aldehydes with β ketoester and urea in the presence of catalytic amounts of PANI-TiO₂ nano catalyst under ultrasound irradiation and solvent-free conditions (Scheme 3).

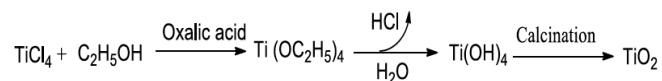
2. EXPERIMENTAL METHOD AND MATERIALS

Melting points of all compounds were determined using Electro thermal 9100. ¹H NMR spectra were recorded on a Bruker DRX-400 Advance instrument with DMSO-d₆ as solvents. All reagents and solvents were purchased from Merck, Fluka and used without further purification.

2.1. Ultrasound Synthesis of TiO₂ Nanoparticles

TiO₂ nanoparticles were synthesized by hydrolysis of titanium tetrachloride (TiCl₄) (0.01 mol) in ethanol under nitrogen atmosphere and oxalic acid (0.001 mol) as additive. The solution was kept at 0°C in an ice-water bath with vigorous stirring as the reaction is exothermic. During the mixing process, white fumes, presumably HCl, were released as a consequence of

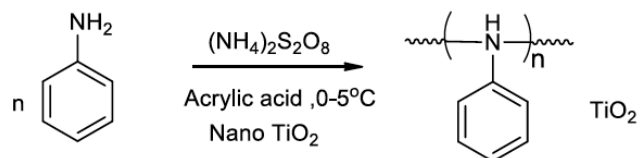
the hydrolysis of TiCl₄ and pH of solution was strongly acidic. The reaction mixture was stirred for 10 minutes and then irradiated for 40 minutes under ultrasound (Ultrasonic frequency: 33 KHz, Ultrasonic power: 100 Watts) to avoid aggregation of nanoparticles and stirred further for 60 minutes at room temperature till a yellow-colored solution of hydrous TiO₂ particles was obtained [16]. Nano particles were then washed with distilled water filtered and dried in an oven at 80°C and calcined at 350°C for four hours in a furnace (Scheme 1).



Scheme 1: Synthesis of TiO₂ nanoparticles.

2.2. Ultrasound Synthesis of Polyaniline - TiO₂ Nanocomposite

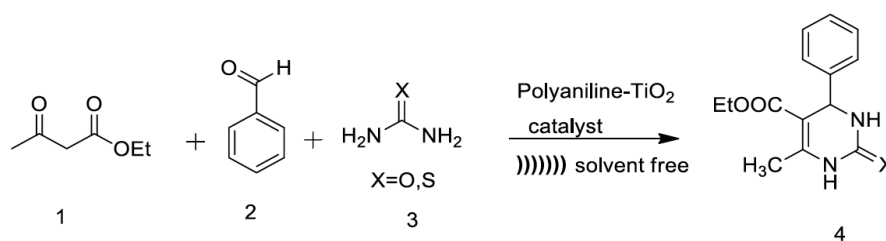
Polymerization reactions were carried out in a well stoppered round bottomed flask containing monomer aniline (0.001mol) under inert atmosphere. To this solution synthesized TiO₂ nanoparticles (0.001mol) were added. Then the flask was sealed with a rubber septum. The solution was degassed with nitrogen for 1 hour. Dopant acrylic acid was added, the oxidizing agent, ammonium persulfate (0.01mol) was dissolved separately in 10 mL de-ionized water and was added drop wise at a rate of approximately 1 mL/min to the above monomer solution containing TiO₂ nano particles under constant stirring at a temperature between 0-5°C. After complete addition of the oxidizing agent, the reaction mixture was kept in an ultra-sonicator for 45 min. The green precipitate of the polymer nanocomposite was isolated by filtration and washed with distilled water until the washing liquid became completely colorless. Finally, the PANI-TiO₂ nano composite was dried under vacuum at 60°C in an oven until a constant mass was achieved. The polyaniline - TiO₂ nanocomposite was characterized by FTIR, XRD and SEM [10-13].



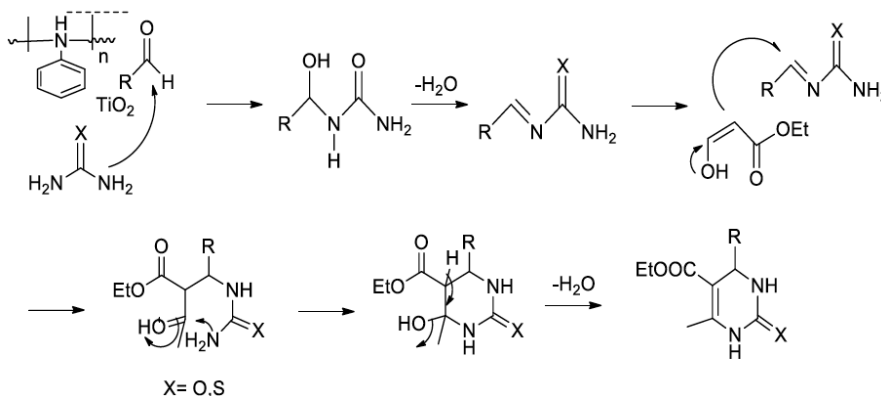
Scheme 2: Synthesis of PANI-TiO₂ nanocomposite.

2.3. Synthesis of Dihydropyrimidinones /Thiones

In a round bottom flask a mixture of the β-dicarbonyl compound (1mmol), aldehyde (1 mmol), urea (1.2



Scheme 3: Synthesis of DHPM's using polyaniline - TiO₂ nanoparticles.



Scheme 4: Probable mechanism for DHPM synthesis using PANI- TiO₂ as a catalyst.

mmol) and polyaniline-TiO₂ nano catalyst (0.005 gm) was taken, under ultrasound irradiation (230 V, Ultrasonic frequency: 33 KHz, Ultrasonic power: 100 Watts) at 45°C. The reaction was monitored by TLC. After completion of the reaction, water was added to the reaction mixture to remove excess of urea and then filtered and washed to get the pure product. Isolated products have almost 99% purity. The purified products were characterized by NMR, IR and mass spectral analysis.

3. RESULTS AND DISCUSSION

3.1. UV-Vis Characterization

UV-Vis absorption spectrum of synthesized TiO₂ nanoparticles is shown in Figure 1a. The spectrum reveals a characteristic sharp absorption peak at

wavelength 365 nm which indicates formation of TiO₂ nanoparticles.

The spectral features of PANI observed in Figure 1b, reveal peak at 320 nm which corresponds to the $\pi - \pi^*$ transition of the benzenoid rings while the sharp peak observed at 620 nm represents the emeraldine salt form of the PANI.

The UV-Vis absorption spectra of TiO₂ doped PANI is shown Figure 1c. Sharp peak at 352 nm indicates PANI-TiO₂. The encapsulation of TiO₂ in PANI resulted in a change in the UV-vis spectrum's morphology.

3.2. FTIR Characterization

Figure 2a shows FTIR spectrum of nano TiO₂ which reveals the broad absorption band at $\sim 3405 \text{ cm}^{-1}$

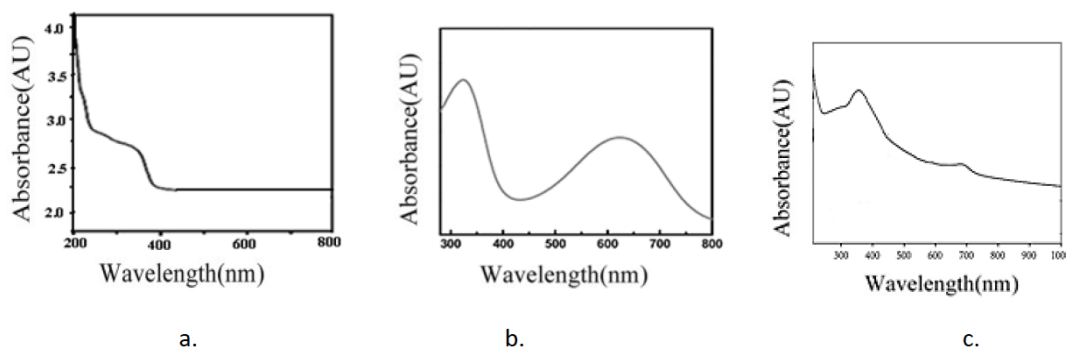


Figure 1: UV-Vis spectrum of a) nano TiO₂ particles b) PANI c) PANI-TiO₂.

corresponding to stretching vibration of O-H bond and peak at $\sim 1638\text{ cm}^{-1}$ which indicates bending vibration of $-\text{O}-\text{H}$ bond. A sharp peak at 1402 cm^{-1} is due to the stretching vibrations of Ti-O-Ti and vibration around 720 cm^{-1} corresponds to the anti-symmetric Ti-O-Ti mode of TiO₂.

The FTIR spectra of the polyaniline doped acrylic acid are given in Figure 2b. The broad and intense peak at $3300\text{--}3100\text{ cm}^{-1}$ is due to $-\text{NH}$ stretching and 1151 cm^{-1} band is due to dopant anion. The strong and intense peak at 1579 cm^{-1} in polymer is observed indicating quinoid ring stretching frequency along with this peak another peak is observed at 1500 cm^{-1} indicating benzenoid ring stretching vibration. Benzenoid and quinoid bands are observed at 1500 cm^{-1} and 1579 cm^{-1} . They are comparatively broad, weak and shifted to the lower wave number. Spectral intensity of these bands is comparatively typical of highly doped emeraldine salt form of polymer. The presence of a weak peak at 1700 cm^{-1} indicates non protonated $-\text{COOH}$ group.

FTIR of polyaniline -TiO₂ shows in Figure 2c, some bands of PANI have shifted due to interactions with

anatase TiO₂ nanoparticles. For example, the bands at 1576 cm^{-1} correspond to the stretching mode of C=N, 1496 cm^{-1} to C=C stretching, and 1310 cm^{-1} is observed due to C-N stretching mode. These changes suggest that C=C, C-N C=N bands become weaker in polyaniline-TiO₂ nanocomposite, while the N-H band becomes stronger. This is probably because of the action of hydrogen bonding between the surfaces of anatase TiO₂ nanoparticles and the N-H groups in polyaniline chain. The results confirm that there is strong interaction between the polyaniline and nanocrystalline TiO₂.

3.3. XRD Analysis

XRD pattern of TiO₂, polyaniline and polyaniline-TiO₂ nanocomposite is shown in Figure 3. XRD analysis of synthesized PANI showed two broad peaks at $2\theta = 20.7$ and 25.5° indicating an amorphous structure of polyaniline as shown Figure 3a.

The diffraction pattern of TiO₂ matches well with literature and is in good agreement with the standard spectrum (JCPDS no. 84-1286). The appearance of sharp diffraction patterns indicates the small size with high

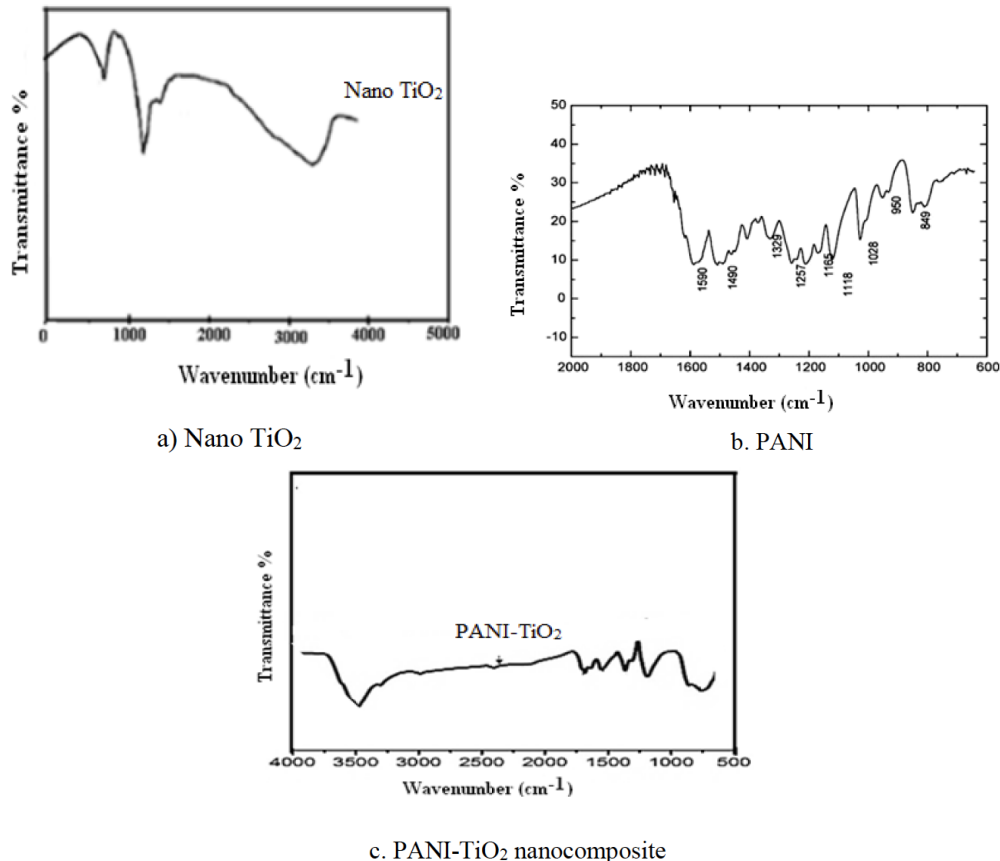


Figure 2: a. FTIR of nano TiO₂ b. PANI and c. PANI-TiO₂ nanocomposite.

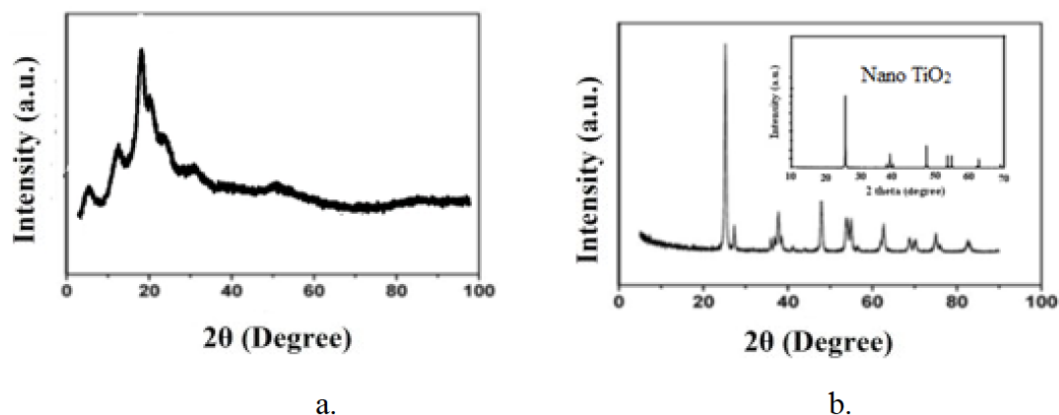


Figure 3: a. XRD pattern of PANI b. nanoTiO₂ and PANI–TiO₂.

purity and crystallinity of the synthesized nano TiO₂. Presence of sharp peaks at 25° and 48° indicates TiO₂ is present in anatase phase. The XRD analysis shows the major reflections between 25° to 70° (2θ values) which indicate TiO₂ nanoparticles average size of 25–30 nm.

XRD pattern of polyaniline-TiO₂ shows diffraction peak at 25°, 40°, 48°, 53° and 68° which are due to (110), (101), (111) and (211) present in nanocomposite which indicates the presence of TiO₂ in polyaniline [JCPDS file no. 21-1276]. The crystalline structure of nanocomposite and obtained results are in good agreement with the literature (Figure 3b).

3.4. SEM Analysis

The surface morphology of TiO₂ was analyzed by SEM and is represented in Figure 4a. It shows that TiO₂ nano particles are highly agglomerated with spherical morphology to form a cluster as observed in SEM micrograph. The PANI exhibits spherical irregular morphology like cauliflower type structure (Figure 4b), while the morphology of PANI-TiO₂ nanoparticles spherical with particle size of about 70 nm (Figure 4c).

3.5. Thermal Stability

The thermal gravimetric analysis (TGA) curves for PANI and its nano-composite are presented in Figure 5. TiO₂ nanoparticles are stable in air and no decomposition takes place in the range 50 to 900°C. On the other hand, polyaniline decomposes sharply at 390°C (Figure 5). On examining the TGA curves, it can be observed that the polyaniline nano-composite has higher thermal stability than pure polyaniline.

3.6. DHPM Synthesis

Scheme 4 illustrates the proposed mechanism for the synthesis of dihydropyrimidinones (DHPM) utilizing PANI-TiO₂ as a catalyst. Initially, the PANI-TiO₂ nanocomposite interacts with the aldehyde carbonyl group. Subsequently, the urea molecule undergoes nucleophilic attack on the carbonyl group, leading to condensation and the formation of a water molecule as a byproduct. This is followed by cyclization, resulting in the formation of dihydropyrimidinone. Post-reaction, the PANI-TiO₂ nanocomposite can be effectively recycled and reused without significant loss of catalytic activity,

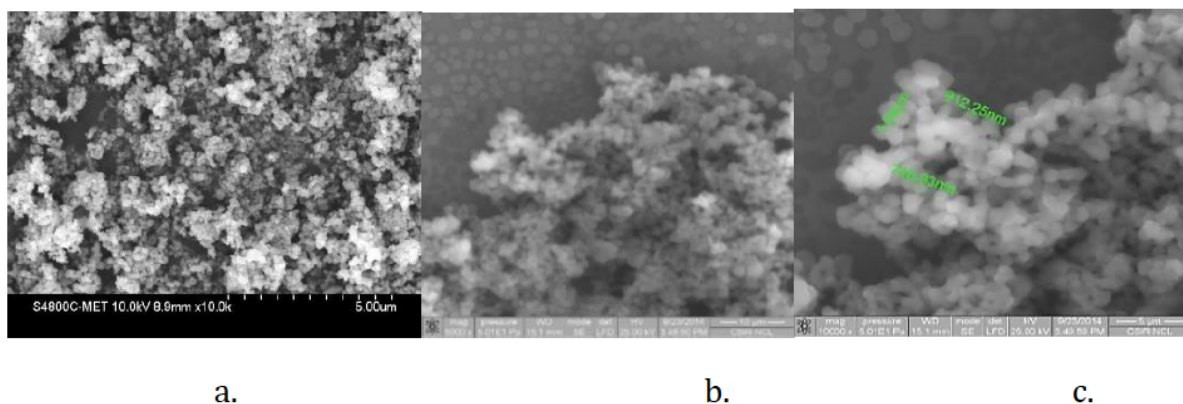


Figure 4: SEM of a) TiO₂ nanoparticle b) PANI c) PANI- TiO₂ nanocomposite.

thus rendering this process both environmentally friendly and cost-effective.

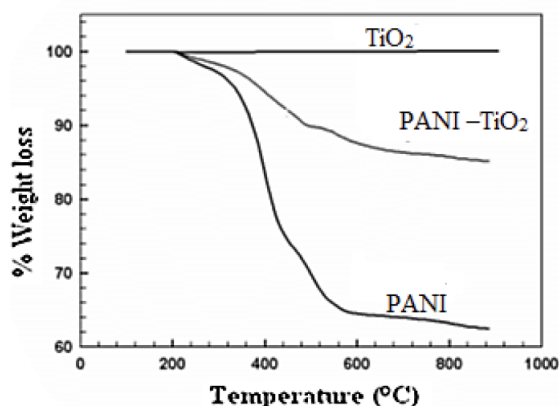


Figure 5: TGA of nano TiO₂, PANI and PANI-TiO₂ nanocomposite.

To investigate the scope of this extension, we subjected a variety of aldehydes to reaction with urea under solventless conditions. The results demonstrate that both electron-donating and electron-withdrawing substituents facilitate the synthesis of the corresponding dihydropyrimidinones (DHPM) under optimized reaction conditions. As detailed in Table 1, the reaction proceeds with high efficiency, yielding DHPM products in commendable yields.

Table 1 clearly indicates that PANI-TiO₂ serves as the most effective catalyst, enhancing the reaction yield compared to traditional synthesis methods employing HCl and ethanol (see Table 1, entries 1, 3, 4, and 5). Additionally, electron-donating substituents on the benzene ring generally produce higher yields (entries 4

and 9) compared to electron-withdrawing substituents (entries 3 and 5).

4. CONCLUSION

Polyaniline decorated TiO₂ nanoparticles were successfully synthesized in situ by chemical oxidative polymerization. The FT-IR and XRD results proved the strong interfacial interaction between the TiO₂ nanoparticles and the polyaniline chain. It is confirmed that the diameter of the resulted PANI-TiO₂ nanoparticles is about 70 nm and the interactions between the two components are strong.

An efficient and environmentally friendly methodology for the synthesis of 3,4-dihydropyrimidin-2-(1H)-ones/thiones has been reported, employing a polyaniline-TiO₂ nanocomposite as a heterogeneous catalyst with high atom economy. This approach is preferable to homogeneous catalysis in terms of environmental impact. The solid, insoluble nature of the PANI-TiO₂ catalyst enables facile removal from the reaction mixture through filtration and facilitates recycling. Moreover, the preparation of the catalyst is straightforward and safe. The process also employs solvent-free conditions, thereby reducing the generation of waste and the use of hazardous substances.

The present protocol is superior in terms of scope for the synthesis of dihydropyrimidinones and thiones, offers several notable advantages over the existing methods, including ease in handling, reusability, thermal stability, environmentally friendly, short reaction times, and operational simplicity.

Table 1: PANI- TiO₂ Promoted Synthesis of Dihydropyrimidinones and Thiones under Solvent Free Condition

Entry	Product	Aldehyde R	X	Ultrasound		M.P.
				Time (min)	Yield (%)	
1	4a	C ₆ H ₅	O	45	92 (78) ^b	202-205
2	4b	PhCH=CH	O	35	95	230-236
3	4c	4-NO ₂ -C ₆ H ₅	O	60	87 (58) ^b	234-236
4	4d	4 NMe ₂ C ₆ H ₄	O	35	92 (86) ^b	256-258
5	4e	4 Cl-C ₆ H ₄	O	47	87 (56) ^b	211-213
6	4f	C ₆ H ₅	S	42	88	203-205
7	4g	PhCH=CH	S	43	86	227-230
8	4h	4-NO ₂ -C ₆ H ₅	S	65	89	153-155
9	4i	4 NMe ₂ C ₆ H ₄	S	40	90	230-233
10	4j	4 Cl-C ₆ H ₄	S	50	86	193-194

Reaction conditions: aldehyde (1 mmol), EAA (1 mmol), urea (1.2 mmol) and PANI-TiO₂ catalyst (0.005 g).

^b Conventional methods of synthesis of DHPM (cat HCl in EtOH, reflux, 18 h).

All products were characterized by IR, ¹H NMR and LCMS.

Spectral Data of Selected Compounds

1) 5-Ethoxycarbonyl-6-methyl-4-phenyl-3,4-dihydropyrimidin-2(1H)-one(4a)

¹H NMR (400 MHz, CDCl₃) δ: 1.10 (t, 3H, *J*=6.88 Hz, OCH₂CH₃), 2.24 (s, 3H, CH₃), 4.06 (q, 2H, *J*=6.88 Hz, OCH₂CH₃), 5.12 (s, 1H, C(4)-H), 7.26-7.30 (m, 5H, C₆H₅), 7.82 (s, 1H, NH), 9.11 (s, 1H, NH); MS (m/e): 261(M+1), 260 (M⁺); IR (KBr) cm⁻¹: 3242, 3115, 1726, 1647, 1600, 1419, 1311, 1091, 783.

2) 5-Ethoxycarbonyl-6-methyl-4-cinnamyl-3,4-dihydropyrimidin-2(1H)-one(4b):

¹H NMR (400 MHz, DMSO-d₆) δ: 1.20 (t, 3H, OCH₂CH₃), 2.23 (s, 3H, vinyl methyl), 4.10 (q, 2H, OCH₂CH₃), 4.85 (d, 1H, C(4)-H), 6.2 (d, 1H, CH=CH), 6.4 (d, 1H, CH=CH), 7.2 (m, 5H, Ar-H), 9.5 (bs, 1H, NH), 10.2 (bs, 1H, NH). MS (m/e): 287(M+1); IR (KBr) cm⁻¹: 3115, 3039, 1710, 1678, 1615, 1250, 750.

3) 5-Ethoxycarbonyl-4-(4-nitro-phenyl)-6-methyl-3,4-dihydropyrimidin-2(1H)-one (4c)

¹H NMR (400 MHz, CDCl₃) δ: 1.1 (t, 3H, OCH₂CH₃), 2.27 (s, 3H, CH₃), 3.98 (q, 2H, OCH₂CH₃), 5.30 (d, 1H, C(4)-H), 7.51 (d, 2H, Ar-H), 7.89 (s, 1H, NH), 8.22 (d, 2H, Ar-H), 9.37 (s, 1H, NH); MS (m/e): 306 (M+1); IR (KBr) cm⁻¹: 3224, 2950, 1745, 1670, 1510, 1340, 1125, 780

4) 5-Ethoxycarbonyl-4-(4-N(CH₃)₂)I-6-methyl-dihydropyrimidin-2(1H)-one (4d)

¹H NMR (400 MHz, DMSO-d₆) δ: 1.18 (t, 3H, *J*=7.6 Hz, CH₃), 2.4 (s, 3H, CH₃), 2.8 (s, 6H, N(CH₃)₂), 4.00 (q, 2H, *J*=7.6 Hz, OCH₂CH₃), 5.02 (d, 1H, C(4)-H), 6.6 (d, 2H, *J*=9.1 Hz, Ar-H), 7.00 (d, 2H, *J*=9.1 Hz, Ar-H), 7.6 and 9.16 (2 bs, 2H, NH); MS (m/e): 304 (M+1); IR (KBr) cm⁻¹: 3200, 3100, 1700, 1685.

5) 5-Ethoxycarbonyl-4-(4-chlorophenyl)-6-methyl-3,4-dihydropyrimidin-2(1H)-one (4e)

¹H NMR (400 MHz, DMSO-d₆) δ: 1.12 (t, 3H, *J*=7.14 Hz, OCH₂CH₃), 2.30 (s, 3H, CH₃), 3.91 (q, 2H, *J*=7.16 Hz, OCH₂CH₃), 5.07 (d, 1H, *J*=2.28, CH), 7.21 (d, 2H, *J*=9.18, Ar-H), 7.69 (d, 2H, *J*=9.18, Ar-H), 7.94 (s, 1H, NH), 9.29 (bs, 1H, NH); MS (m/e): 295 (M+1); IR (KBr) cm⁻¹: 3225, 1720, 1615.

6) 5-Ethoxycarbonyl-4-(4-chlorophenyl)-6-methyl-3,4-dihydropyrimidin-2(1H)-one (4f)

¹H NMR (DMSO-d₆) δ: 1.12 (t, 3H, *J* = 7.14 Hz, -OCH₂CH₃), 2.30 (s, 3H, -CH₃), 3.91 (q, 2H, *J*=7.16 Hz, -OCH₂CH₃), 5.70 (d, 1H, *J* = 2.28, -CH), 7.21 (d, 2H, *J* =

9.18, Ar-H), 7.69 (s, 1H, -NH), 7.94 (d, 2H, *J* = 9.18, Ar-H), 9.16 (s, 1H, -NH). MS (m/e): 297 (M+1); IR (KBr, cm⁻¹): IR (KBr, cm⁻¹): 3225, 1720, 1615.

7) 5-Ethoxycarbonyl-4-(4-phenyl)-6-methyl-3,4-dihydropyrimidin-2(1H)-thione (4g)

¹H NMR (DMSO-d₆): δ 1.19 (t, *J*=7.3 Hz, 3H, CH₃), 2.27 (s, 3H, CH₃), 4.08 (q, *J*=7.3 Hz, 2H, -OCH₂), 5.22 (s, 1H, CH), 7.23 (m, 5H, Ar), 9.25 and 9.9 (2s, 2H, 2brs. NH); MS (m/e): (M+1)293; IR (KBr, cm⁻¹): 3244, 3115, 1727, 1647, 1600, 1419, 1311, 1091, 783.

8) 5-Ethoxycarbonyl-4-(4-nitrophenyl)-6-methyl-3,4-dihydropyrimidin-2(1H)-thione (4h)

¹H NMR (DMSO-d₆): δ 1.13 (t, 3H, CH₃-CH₂O), 2.31 (s, 3H, -CH₃), 3.99 (q, 2H, -OCH₂), 5.22 (s, 1H, CH), 7.56 (d, 2H, ArH), 7.90 (s, 1H, -NH), 8.11 (d, 2H, ArH), 9.39 (s, 1H, NH) MS: (M+1); 338; IR (KBr) cm⁻¹: 3226, 2950, 1745, 1670, 1510, 1340, 1127, 782.

9) 5-Ethoxycarbonyl-4-(4-N(CH₃)₂)I-6-methyl-3,4-dihydropyrimidin-2(1H)-thione (4i):

¹H NMR (400 MHz, DMSO-d₆) δ: 1.20 (t, 3H, *J*=7.6 Hz, CH₃), 2.25 (s, 3H, CH₃), 2.87 (s, 6H, N(CH₃)₂), 4.00 (q, 2H, *J*=7.6 Hz, OCH₂), 5.18 (d, 1H, C(4)-H), 6.62 (d, 2H, *J*=9.1 Hz, Ar-H), 7.19 (d, 2H, *J*=9.1 Hz, Ar-H), 9.80 (bs, 1H, NH), 10.2 (bs, 1H, NH); MS (m/e): 320 (M+1); IR (KBr) cm⁻¹: 3196, 1640, 1552, 1475, 1191.

10) 5-Ethoxycarbonyl-4-(4-chlorophenyl)-6-methyl-3,4-dihydropyrimidin-2(1H)-thione (4j)

¹H NMR (DMSO-d₆) δ: 1.10 (t, 3H, *J* = 7.01 Hz, -OCH₂CH₃), 2.29 (s, 3H, -CH₃), 2.26 (3H, s, -CH₃) 4.00 (q, 2H, *J*=7.01 Hz, -OCH₂CH₃), 5.16 (d, 1H, -C(4)H), 7.22 (d, 2H, *J* = 7.04 Hz, Ar-H), 7.43 (d, 2H, *J* = 7.04 Hz, Ar-H), 10.40 (br s, 1H, -NH), 9.68 (br s, 1H, -NH). MS: m/e (M+1) 311 ((M+1) IR (KBr) cm⁻¹: 3225, 1720, 1615.

ACKNOWLEDGEMENT

The authors are grateful to the Savitribai Phule Pune University, C-MET and NCL, Pune for characterization and activity. We also thank Nowrosjee Wadia College, Pune for providing lab facility.

REFERENCES

- [1] Kappe CO. Recent Advances in the Biginelli Dihydropyrimidine Synthesis. New Tricks from an Old Dog. *Acc Chem Res* 2000; 33: 879-888. <https://doi.org/10.1021/ar000048h>
- [2] Ugi I, Domling A, Horl W. Multicomponent Reactions in Organic Chemistry. *Endeavour New Ser* 1994; 18: 115-122. [https://doi.org/10.1016/S0160-9327\(05\)80086-9](https://doi.org/10.1016/S0160-9327(05)80086-9)

- [3] Kappe CO, Fabian W. Synthesis and Reactions of Biginelli Compounds. Conformational Analysis of 4-aryl-dihydropyrimidine Calcium-Channel Modulators—a Comparison of *ab-initio*, Semi empirical and X-ray Crystallographic Studies. *Tetrahedron Lett* 1997; 53: 2803-2816.
- [4] Hurst EW, Hull R. Two New Synthetic Substances Active against Viruses of the Psittacosis-Lymphogranuloma-Trachoma Group. *J Med Pharm Chem* 1961; 3: 215-229. <https://doi.org/10.1021/jm50015a002>
- [5] Jalali M, Mahdavi M, Memarian HR, Ranjbar M, Soleymani M, Fassihi A, Abedi D. Antimicrobial Evaluation of Some Novel Derivatives of 3,4-Dihydropyrimidine-2(1H)-one. *Res Pharm Sci* 2012; 7: 243-247. <https://doi.org/10.1016/j.bmcl.2008.10.063>
- [6] Kapoor TM, Mayer TU, Conghlin ML, Mitchison JJ. Probing Spindle Assembly Mechanisms with Monastrol, a Small Molecule Inhibitor of the Mitotic Kinesin Eg5. *J Cell Biol* 2009; 75-988. <https://doi.org/10.1083/jcb.150.5.975>
- [7] Polshettiwar V, Varma RS. Biginelli Reaction in Aqueous Medium: a Greener and Sustainable Approach to Substituted 3,4-dihydropyrimidin-2(1H)-ones. *Tetrahedron Lett* 2007; 48: 7343-7346. <https://doi.org/10.1016/j.tetlet.2007.08.031>
- [8] Kappe CO. Biologically active dihydropyrimidones of the Biginelli-type a literature survey. *Eur J Med Chem* 2000; 35: 1043-1052. [https://doi.org/10.1016/s0223-5234\(00\)01189-2](https://doi.org/10.1016/s0223-5234(00)01189-2)
- [9] Chabukswar VV, Handore KN, Bhavsar SV, Horne AS, Dallavalle S, Gaikwad VB, Mohite KC. Conducting Polyaniline is an Efficient Catalyst for Synthesis of 3,4-dihydropyrimidin-2(1H)-one Derivative under Solvent-free Conditions. *Macromol Sci Pt A Pure Appl Chem* 2013; 50: 411-415. <https://doi.org/10.1080/03602559.2013.877930>
- [10] Hidalgo D, Bocchini M, Fontana M, Saracco G. Green and Low-cost Synthesis of PANI-TiO₂ Nanocomposite Mesoporous Films for Photo electrochemical Water Splitting. *RSC advances* 2015; 5: 49429-49438. <https://doi.org/10.1039/C5RA06734K>
- [11] Chabukswar VV, Handore KN, Bhavsar SV, Pande N, Chhattise PK, Sharma SB, Dallavalle S, Gaikwad VB, Mohite KC. Polyindole-ZnO Nanocomposite: Synthesis, Characterization and Heterogeneous Catalyst for the 3,4-Dihydropyrimidinone Synthesis under Solvent-free Conditions. *Polymer Plastic Technology and Engg* 2014; 53: 734-741. <https://doi.org/10.1080/03602559.2013.877930>
- [12] Yucheng L, Yalin L, Zhifeng R. Review on Photocatalysis of Titanium Dioxide Nanoparticles and their Solar Applications. *Nano Energy* 2013; 2: 1031-1045. <https://doi.org/10.1016/j.nanoen.2013.04.002>
- [13] Pawar SG, Patil SL, Chougule MA, Raut BT, Sen S, Patil VB. Camphor Sulfonic Acid Doped Polyaniline-titanium Dioxide Nanocomposite Synthesis, Structural, Morphological, and Electrical Properties. *Int J Polym Mat* 2011; 60: 979-987. <https://doi.org/10.1080/00914037.2011.553848>
- [14] Patel HA, Sawant AM, Rao VJ, Patel AL, Bedekar AV. Polyaniline Supported FeCl₃: An Effective Heterogeneous Catalyst for Biginelli Reaction. *Catal Lett* 2017; 147: 2306-2312. <https://doi.org/10.1007/s10562-017-2139-9>
- [15] Zhang L, Liu P, Su Z. Preparation of PANI-TiO₂ Nanocomposites and their Solid-phase Photocatalytic Degradation. *Polym Degrad Stab* 2006; 91: 2213-2219. <https://doi.org/10.1016/j.polymdegradstab.2006.01.002>
- [16] Handore KN, Walunj D, Chhattis P, Chabukswar A, Mohite K, Dallavalle S, Bahule B, Chabukswar V. Ultrasound Synthesis of Polyindole-TiO₂ Nanocomposite and Evaluation of Anti-bacterial Activity. *Polymer Plastic Technology and Engg* 2017; 56: 1259-1266. <https://doi.org/10.1080/03602559.2016.1163581>
- [17] Handore K, Chabukswar V, Pawar D, Dallavalle S. Ultrasound Assisted Solvent free, Synthesis of 3,4-Dihydropyrimidines-2(1H)-ones Using Polyindole as a Recyclable Catalyst. *Polymer Plastic Technology and Engg* 2021; 60: <https://doi.org/10.1080/25740881.2020.1811313>
- [18] Kondo HT, Kuwahara MT, Shimomura M. Electrochemical Polymerization of Aniline in the Presence of Poly (acrylic acid) and Characterization of the Resulting Films. *Polymer* 2012; 53: 223-228. <https://doi.org/10.1016/j.polymer.2011.11.038>
- [19] Olad A, Ramazani Z. Preparation, Characterization and Anticorrosive Properties of Polyaniline Nanotubes. *Int J Polym Mater* 2012; 61: 949-962. <https://doi.org/10.1080/00914037.2011.610063>
- [20] Chaudhari SB, Mandot AA, Patel BH. Effect of Nano TiO₂ Pre-treatment on Functional Properties of Cotton Fabric. *International Journal of Engineering Research and Development* 2012; 1: 24-29.
- [21] Wei Q, Yu L, Mather RR, Wang X. Preparation and Characterization of Titanium Dioxide Nanocomposite Fibers. *J Mater Sci* 2007; 42: 8001-8005. <https://doi.org/10.1007/s10853-007-1582-1>
- [22] Song H, Li C, Lou Z, Ye Z, Zhu L. Effective Formation of Oxygen Vacancies in Black TiO₂ Nanostructures with Efficient Solar-driven Water Splitting. *ACS Sustain Chem Eng* 2017; 5: 8982-8987. <https://doi.org/10.1007/s10853-007-1582-1>
- [23] Hu YA. Highly Efficient Photocatalyst-Hydrogenated Black TiO₂ for the Photocatalytic Splitting of Water. *Angew. Chem Int Ed* 2012; 51: 12410-12412. <https://doi.org/10.1002/anie.201206375>
- [24] Ding Q, Yang Q, Wu T, Zhu W, Ouyang X, Yang Q, Liu L, Wang Y. TiO₂/InVO₄ *n-n* Heterojunction for Efficient Ammonia Gas Detection and their Sensing Mechanisms. *Journal of Materials Science* 2019; 54: 13660-13673. <https://doi.org/10.1007/s10853-019-03868-z>
- [25] Fox MA, Dulay MT. Heterogeneous photocatalysis. *Chemical Reviews* 1993; 93: 341-357. <https://doi.org/10.1021/cr00017a016>
- [26] Hashemabad NZ, Shabanpour B, Azizi H, Ojagh SM, Alishahi A. Effect of TiO₂ Nanoparticles on the Antibacterial and Physical Properties of Low-Density Polyethylene Film. *Polymer plastic Technology and Engineering* 2017; 56: 1516-1527. <https://doi.org/10.1080/03602559.2016.1278022>

Received on 19-09-2024

Accepted on 25-10-2024

Published on 29-11-2024

<https://doi.org/10.6000/1929-5995.2024.13.25>© 2024 Handore *et al.*

This is an open-access article licensed under the terms of the Creative Commons Attribution License (<http://creativecommons.org/licenses/by/4.0/>), which permits unrestricted use, distribution, and reproduction in any medium, provided the work is properly cited.